Time Resolved Synchrotron Radiation X-Ray Topography Study of Surface Acoustic Waves Propagation.

Bernard Capelle, Yves Epelboin, Jacques Détaint, Alain Soyer, Jürgen Härtwig*

Institut de Minéralogie et de Physique des Milieux Condensés (IMPMC), UMR 7590 CNRS. Universités Paris VI et Paris VII. 140, rue de Lourmel 75015 Paris. France.

*European Synchrotron Radiation Facility (ESRF). X-ray Optics Group.

6, rue Horowitz BP 220, 38043 Grenoble. France.

***Abstract*— The purpose of this contribution is to study several phenomena influencing the formation of X-rays diffraction images of SAW propagating on crystals so to be able to use them to obtain further information about the SAW. We consider particularly new contrasts appearing in white beam section topographs made with low or large amplitude SAW. The first ones can bring information about propagation at different depth and the second allows a measurement of the amplitude of the SAW.**

I. INTRODUCTION

X-Ray topography is a very sensitive method to image strain fields in crystals. Many contributions using this technique were devoted to image surface acoustic waves (SAW) in devices employing standing waves (most often SAW resonators) or progressive waves (mostly transversal filters) [1 to 5] The periodic nature of the synchrotron radiation (constituted of very short X-Ray pulses) and the very small wave length of the X-rays has allowed making much better, time resolved (or stroboscopic) observations of progressive SAW. The main purpose of this communication is to present and to discuss several feature of the time resolved synchrotron radiation X-Ray topography that allow to better study the actual acoustic field existing in SAW devices.

The SAW of infinite extension may have only two displacement components when particular symmetries exist (such as in YZ LiNbO3) or, more often, three that decay in the substrate. However the displacement field existing in actual devices can be quite different of those of theoretical SAW due to the effect of the finite dimensions, of the bus lines, of apodization, etc… It is generally difficult to compute very accurately the components of the actual displacement of real devices but they are quite easily imaged using time resolved synchrotron x-ray topography that has a great resolution and allow studying all the components of the SAW often separately. However, most often only the component normal to the surface is imaged since all the components are coupled and since most of the desirable information is generally obtained doing so. In this paper we will presents some features observed in "section" and "translation" images of SAW of moderate and of large amplitude, made using white beams or monochromatic radiations. To our knowledge it is the first time that such features that affect the formation of the diffraction images are observed. The observations made with SAW of large amplitude have allowed establishing a technique to determine the variations of the amplitude of the SAW in a device. Some other effects occurring in devices submitted to a very large excitation were also observed and are reported (direct observation of a nonlinear behavior).

II. IMAGING THE NORMAL COMPONENT OF SAW.

Experimental set-up

Most of the results presented here after were obtained during experiments made on beam lines ID19 and BM05 of the European Synchrotron Radiation Facility (ESRF) at Grenoble (France) with the objective to better understand the mechanism of diffraction in crystals highly distorted by acoustic waves. In these experiments several diffraction configurations and different high accuracy diffractometers were used. The very low divergence achieved on these beam lines and the quality of the monochromators used have allowed to obtain image than can be compared to numerical simulations to further understand the diffraction mechanisms implied from a theoretical point of view (this is being done and will be reported elsewhere). A few translation topographs presented here after were obtained some time ago at LURE (Orsay- France). In most case the Bragg geometry was used to image the normal component of the SAW using a diffraction vector exactly or approximately normal to the surface of the device (Figure 1). The names "section" and "translation" topographs refer to the Lang method using conventional X-ray

978-1-4244-3510-4/09/$25.00 ©2009 IEEE

sources that need to be limited to very thin beam to reduce to divergence. In this case, a translation of the crystal and of the film is used to image a larger surface of the crystal. Section images are obtained when no translation are used.

The frequency of the signal exciting the SAW is produced from an internal signal of the synchrotron to be an exact multiple of the revolution frequency of the synchrotron. Its phase can be continuously adjusted so that the instant of maximum of strain associated with the SAW can be in phase or out of phase with the X-ray pulses delivered by the synchrotron.

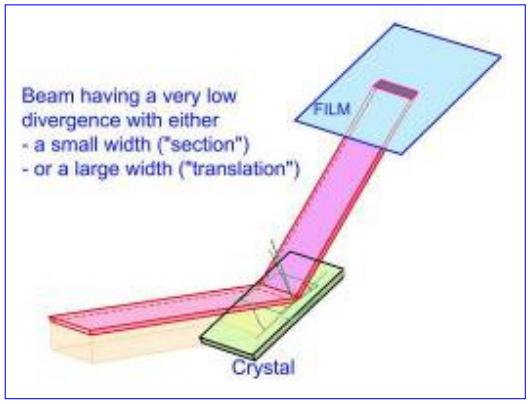

Figure 1. Bragg diffraction geometry.

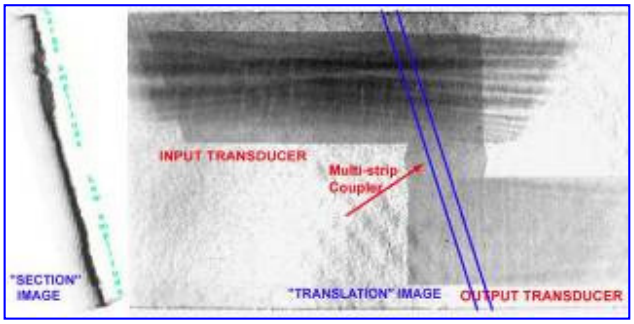

Figure 2. Example of "section" and "translation" topographs , (03.0) reflexion , incidence angle θ=25°. The device imaged is a very performing SAW filter used in professional TV equipments made on Y-Z $LiNbO_3$.

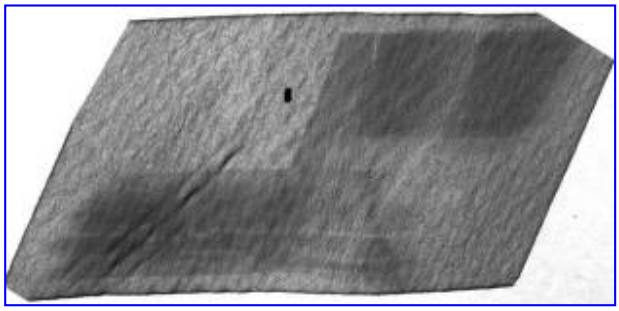

Figure 3. Image obtained with a similar filter and a smaller incidence angle (θ=15°), white beam radiation (03.0 reflexion).

During previous experiments [3] we have observed that the "optimal" incidence angles to get "good" translation images of SAW with white radiations were situated at quite large values (25-30°) in the case of wave propagating on Y-Z $LiNbO_3$ ((03.0) reflexion). This results, in parts, of the fact that in the images made with small incidence angles, the small wave length radiation used penetrate significantly more in the substrate and give contrasts that corresponds to the numerous defects existing in this material (dislocation, sub-grain boundary, etc..) and probably also of more intricate (theoretical) factors. In figure 3, an image of a similar filter obtained with an incidence angle of 15° is presented. We can observe more defects including those due to the striations made at the back of plate to suppress the bulk wave also generated by the transducers. During these experiments, it was also observed that the radiation diagram of the excited transducer (using apodization) was changing rapidly as the frequency of the exciting signal is changed in the pass band). This is illustrated in figure 4. The filters studied are made of two apodized transducers that are disposed in two separated tracks, to avoid the triple transit echo. A multi-strip coupler is used to transfer the SAW from the excited transducer to the second one.

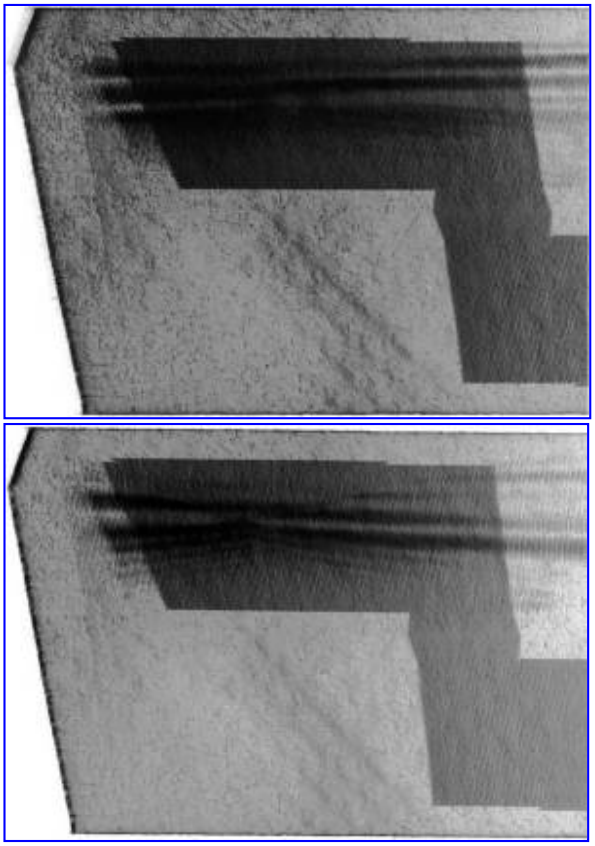

Figure 4. Variation of the radiation diagram of the excited transducer with the excitation frequency . (Same type of filter made on Y-Z $LiNbO_3$,(03.0) reflexion, white bean radiation, incidence angle 25°)

It transform, with a total efficiency, the SAW that are in phase with it spatial position in electrical signals that are transformed back to SAW in the second track to excite the second transducer. It is possible to observe in the topographs that it generates straight crested wave. The fraction of the

SAW emitted by the first transducer that are not in phase with the multi-strip coupler are transmitted and then absorbed. More details can be observed in figure 5.

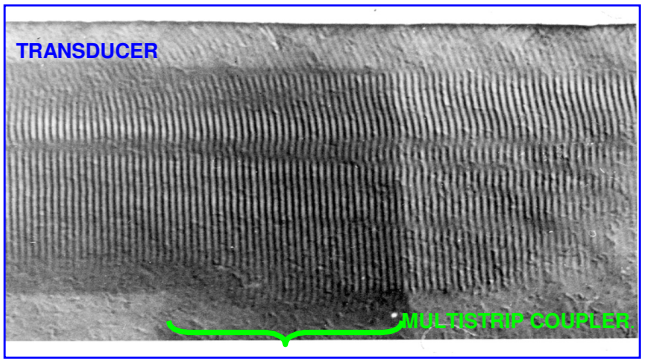

Figure 5. Details of the SAW generated by the input transducer , when they cross the multistrip coupler.

III. PARTICULAR FEATURES OBSERVED IN IMAGES OBTAINED WITH LOW AMPLITUDE SAW.

In the section topographs made under the multi-strip coupler where straight crested SAW are generated, we have observed unexpected contrasts extending much more than the expected width of the section image (figure 6 and 7). In order to obtain more details the filter was rotated in his plane by about 20° (see figure 2).

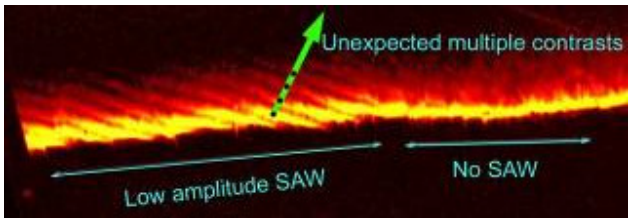

Figure 6. "False color" image showing details of the low density parts of the original section image of figure 7.

In fact five to six successive images of the SAW with decreasing densities are obtained while the first one, much denser, produced by the SAW is larger than the corresponding image of the non-vibrating part of substrate.

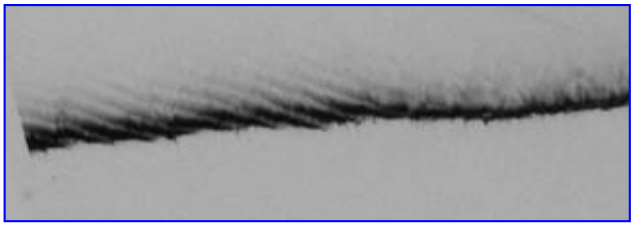

Figure 7. Original section image taken under the multistrip coupler. (03.0) Reflexion . The incident beam has a width of the order of 35 µm which correspond to about one SAW wave length on the substrate (# 100 µm) depending on the frequency used.

Several explanations are possible for the successive images appearing in figure 6. One is related to the role of the harmonics of the used wave length (λ=1.25Å for θ=25°) that can image parts of the saw situated at depth increasing with the harmonic rank. Another explanation can be related to the multi-trajectories diffraction than can exist in deformed crystal [6][7]. They were predicted and observed in crystals curved by a constant strain gradient. This latter case is very similar to what happens near the extremes of a sinusoidal wave.

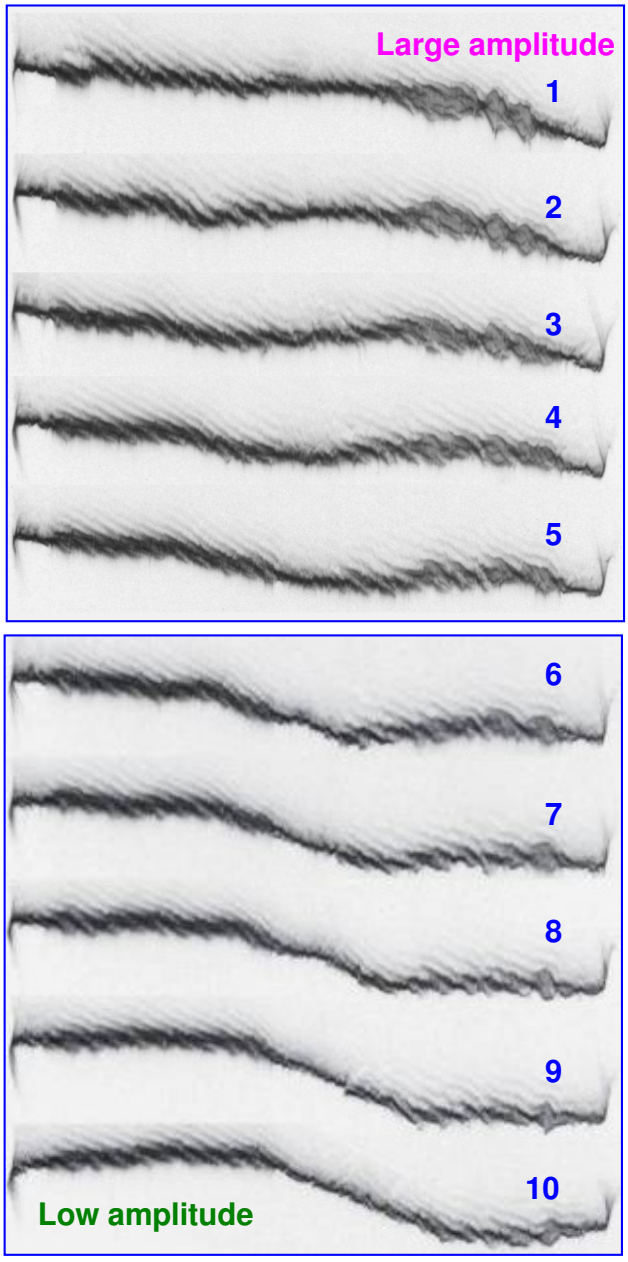

Figure 8. Successive sections images spaced by 0.5 mm taken in the multi-strip coupler region and at the beginning of the second transducer (figure 2).

In figure 8, the section cut both tracks of the filter so that they contain contrasts characteristic respectively of large and low amplitude SAW (the ratio being of the order of 15 dB). The contrasts concerning the low amplitude SAW are of the

same nature as those presented in figure 6 and 7 and they does not vary very much between the different sections (except for some long range distortions due to the curvature of the substrate). The contrasts concerning the large amplitude SAW are very different and they will be discussed in a following paragraph.

Monochromatic images of moderate amplitude SAW.

Image obtained with a monochromatic beam limited by a slit were made of SAW generated by uniform transducers on ST Quartz and Y-Z $LiNbO_3$. No unexpected contrasts were observed (figure 9 and 10) in these experiments made with conditions limiting the amplitude of harmonics (mainly by the choice of the energy (20 Kev)).

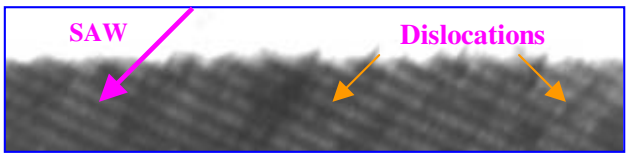

Figure 9. Image of SAW on ST quartz, the contrasts nearly orthogonal to the SAW wave fronts are due to the dislocations present in this substrate. (01.-1) reflexion, 20 KeV, frequency =11.361376 MHz

On these figures, it is possible to observe that, as in figure 7, the parts of the SAW presenting the largest strain gradient (and the dislocations) tends to give enlarged images in the upper regions of the topographs where the incident beam is limited by a slit.

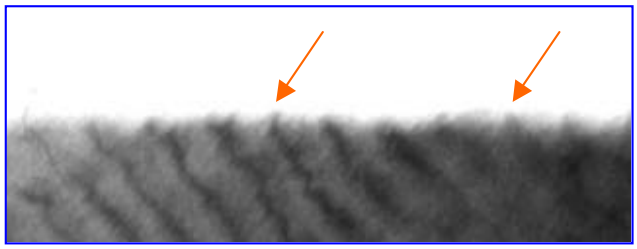

Figure 10. Image of SAW on Y-Z $LiNbO_3$ (03.0) reflexion, 20KeV, , frequency =11.361376 MHz

It should be noticed that these monochromatic images obtained with a beam having a very limited spectra are considerably more sensitive to the defects (Figure 9 and 11) and to the curvature of the substrates (figure 10) than those obtained with a white beam.

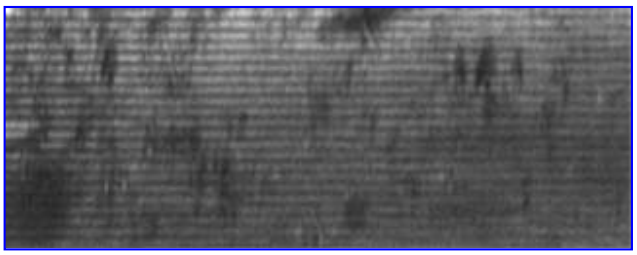

Figure 11. SAW generated on a commercial ST Quartz substrate by an uniform transducer.

Figure 11 represent a larger part of the translation image of an ST quartz delay line using a uniform transducer that produces straight crested waves. It should be noticed that many defects exist in the commercial substrate used in this experiment (mainly dislocations). The width of the rocking curves of ST quartz and Y-Z lithium niobate were measured with and without SAW on the samples considered in figure 9 and 10 and on some other samples.

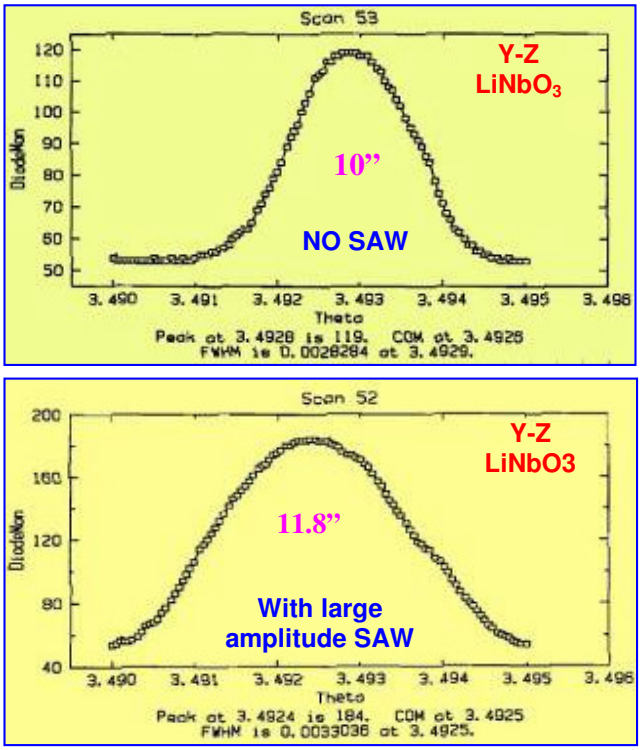

Figure 12. Rocking curves of Y-Z $LiNbO_3$ with and without SAW.

The width stays constant in the case of quartz for all the values of the excitation voltage from zero, but at a value (#7.5 second of arc) which is larger than expected (this seems to be due to the numerous defects present in the commercial substrate used and to the curvature of the plate). For lithium niobate, the width remains constant for a large range of excitations but begin to increase when large voltages are applied to the transducer (Figure 12). In this case, the estimation of the variation should probably take into account the effective output spectra of the monochromator. It should be noticed that the amplitude of the SAW on ST quartz is much smaller, at equal excitation than for lithium niobate due to the smaller coupling coefficient.

On the whole, the results of the different experiments tend to favor the hypothesis that the multiple contrasts observed with a white beam are due to the harmonics of the used wave length. In order to formulate a definitive conclusion numerical simulations of section images in different conditions are being made using a proved technique [8]. In the case of a confirmation of the hypothesis, it will be possible to use the observed multiple contrasts to get new information about the propagation of the SAW at different depth.

IV. IMAGES OF LARGE AMPLITUDE SAW.

We have already noticed in figure 8 that new features appear in the images of large amplitude SAW. These new contrast appearing in the central part of the section image have a much larger width than those observed for low amplitude SAW, they extend on both side of the projection of the slit. More over their width is dependant (nearly proportional) to the excitation voltage and to the distance between the sample and the film. A typical observation is presented in figure 13 where it can be observed that the central part of these new contrasts are some how blurred. They appear to be of similar nature as those encountered in bulk wave device strongly excited [9].

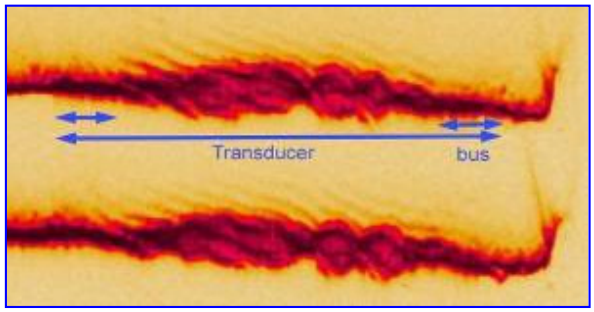

Figure 13. New type of constrasts appearing at large excitation voltage

For the bulk waves we have shown that these kinds of contrasts appear progressively when the strains due to the vibration mode becomes very large. Then, the width of the section images that should, in the frame of the dynamical theory of diffraction, remain constant, begins to grow in the regions corresponding to the largest strains. Simultaneously, the width of the central part of the image becomes dependant of the distance at which is placed the film (figures 14-15).

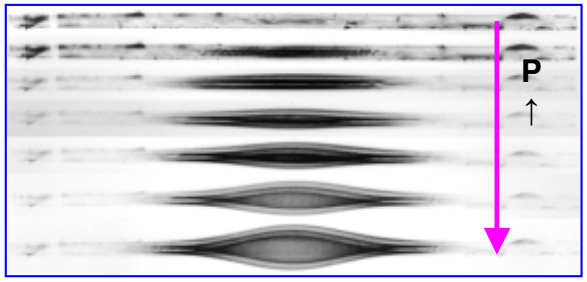

Figure 14. Influence of the excitation level on the section image (AT Quartz 5th overtone resonator . Fr=6.390MHz, –21.0 reflexion, Laue Geometry)

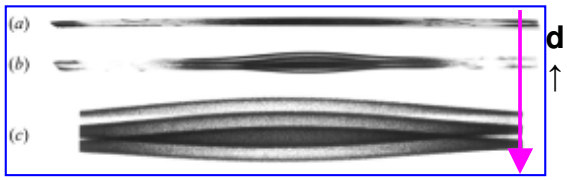

Figure 15. Influence of the film - sample distance on the recorded image (a:4cm , b:70cm ,c: enlargment of b)

It was also shown that this kind of image constitute a "section" map of the vibration amplitude of the device (figure 16).

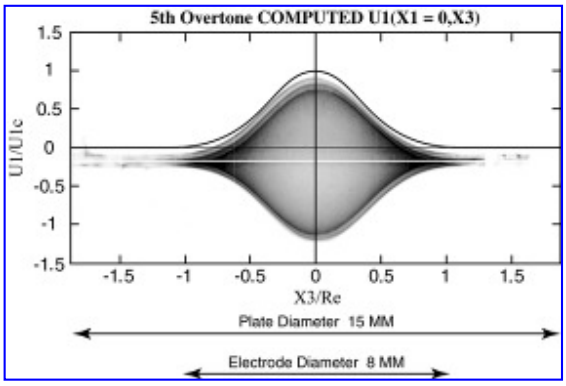

Figure 16. Comparison of the computed mode shpe and of the experimental section image (AT quartz 5th overtone, d=140 cm)

In both cases (Laue or Bragg geometry), the explanation is the same: when the lattice distortions are so large that the hypothesis of the dynamical theory are no more fulfilled, the interactions between the refracted and the diffracted beam uncouple (except very locally) and the image becomes sensitive to the local angle variations of the diffraction vector (figure 17). So that a divergent diffracted beam is produced that is function of these rotations (kinematical image), so that the mode shape is imaged (figures 16-18).

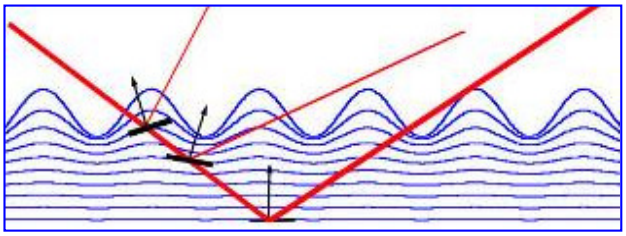

Figure 17. Mechanism of formation of the images under large excitation (Bragg case)

This allows to obtain cartography of the normal displacement in the SAW devices and particularly to analyze the actual lateral variations of the normal displacement along the aperture of the transducer. To this end, successive sections are made under high excitation, to obtain a greater sensitivity; the film is placed at a larger distance than usual for conventional topographs. An example of the observations made is given in figure 18 where the SAW field existing under the excited transducer was imaged using 10 sections images taken at an interval of 0.5mm, the film being placed at 80 cm of the filter (white beam, (03.0) reflexion, incidence angle 25°).

In this figure, we observe a fast variation of the mode shape produced by the apodized transducer. The variations of the amplitude observed in figure 18 are, in fact, associated with phase variations. These phase variations are observed in translation images (see, for example, figure 5), so that a complete characterization of the SAW existing in real devices can be made using section and translation topographs.

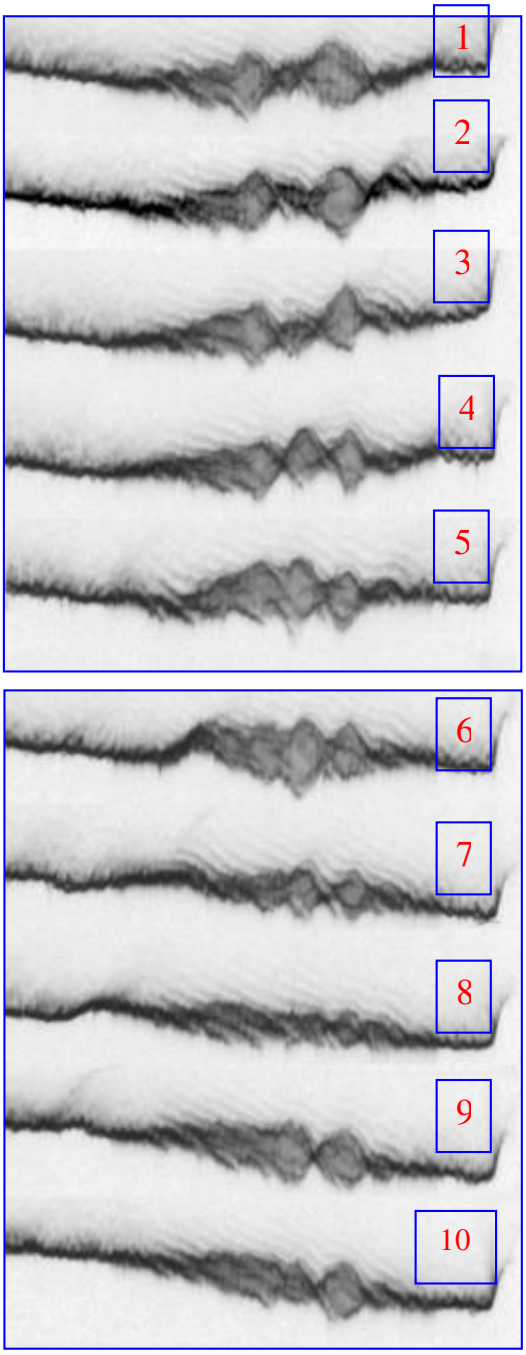

Figure 18. Variations of the mode shape (latera variations of the amplitude) under the excited transducer. (Y-Z LiNbO3, (03.0) reflextion, white beam)

In the experiments made using a monochromatic beam these contrasts were not observed, instead we have observed, at the highest excitation levels, a progressive deformation of the image of the wave (corresponding to a non linear behavior) and then, the apparition of harmonics of the SAW (figure 19). The apparition of the second harmonic of the SAW (and some times of higher harmonics) is not uniform in the device and it appears to be very sensitive to local properties (electrical conditions, material defects or curvature, etc…). This can be observed in figure 19.

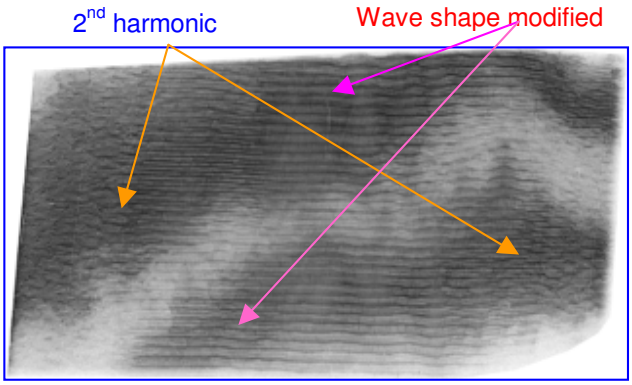

Figure 19. Effects observed with a monochromatic beam for very high excitation (Y-Z LiNbO3, uniform transducer,(03.0) reflexion 20KeV)

V. CONCLUSION

The experiments reported have led to a better understanding of mechanism of formation of the diffraction images of crystals distorted by SAW. The multiples contrasts appearing in section image of SAW devices, obtained with a white beam, seems to be mostly due to the harmonics of the used X-rays wave length. A method using the particularities of the diffraction by highly distorted crystal was set-up to image the amplitude variations of SAW across a device.

Acknowledgments:

The authors acknowledge the very helpful contributions of Adrian Balan and Alain Jeanne Michaud to this study and to the obtainment of the many topographs presented in this paper.

References

[1] D.V. Roshchupkin, H.D. Roshchupkina, D.V. Irzhak. IEEE Trans. on Ultrasonics, Ferroelectrics and Frequency Control, vol. 52, no. 11, p.2082-2087 (2005).

[2] R.W. Whatmore, P.A. Goddard, B.K.Tanner, Proc. 1982 IEEE Ultrasonics Symposium p. 363-366

[3] A. Zarka, B. Capelle, J. Detaint, J. Schwartzel, J.M. Hode. Proc.1993 IEEE Int. Freq. Control Symp. p. 632.

[4] W. Sauer, M. Streibl, T. H. Metzger, A. G. Haubrich, S. Manus, A. Wixforth, J. Peisl, A. Mazuelas, J. Härtwig and J. Baruchel. Proc.1999 IEEE Ultrasonics Symp. p. 69-72.

[5] R. Tucoulou, F. de Bergevin, O. Mathon, and D. V. Roshchupkin, Phys. Rev. *B*, vol. 64, pp. 134108(1–9), 2001.

[6] C. Malgrange, J.Gronkowski J.Phys.Stat. Sol. (a) v.85 p.389-397 (1984)

[7] A. Authier. Dynamical theory of X-ray diffraction IUCR Oxford Science Publication (2001)

[8] V. Mocella, Y.Epelboin.J.Appll. Cryst. V.32; p. 154-159 (1999).

[9] B.Capelle, J.Detaint, Y.Epelboin. J. Appl. Cryst. V. 34, p. 625-629 (2001).